Protons in Oxides [and Discussion]

C. R. A. Catlow, P. S. Baram, S. C. Parker, J. Purton, K. V. Wright, R. Jones, M. Symons and A. M. Stoneham

Phil. Trans. R. Soc. Lond. A 1995 **350**, 265-276
doi: 10.1098/rsta.1995.0013

Protons in oxides

By C. R. A. Catlow[1], P. S. Baram[2], S. C. Parker[2], J. Purton[2]
and K. V. Wright[3]

[1] *Davy Faraday Research Laboratory, The Royal Institution of Great Britain,*
21 Albemarle Street, London W1X 4BS, U.K.
[2] *Department of Chemistry, University of Bath, Claverton Down,*
Bath BA2 7AY, U.K.
[3] *Materials Science Centre, University of Manchester and UMIST,*
Grosvenor Street, Manchester M1 7HS, U.K.

We review the nature of the defects and defect reactions involved in the incorporation of water and hydrogen in oxides and silicates. We describe the role of computational techniques in investigating the structures and energies of hydrogen containing defects in these materials.

1. Introduction

The presence of water and of hydrogen containing defects is known often to have a controlling influence on both the chemical and physical properties of oxide and silicate materials; examples range from the role of Brønsted acidic hydroxyl groups in catalytic aluminosilicates (Thomas 1993) through solid state proton conduction (Iwahara 1992) to the crucial yet poorly understood mechanisms of the reaction of water with quartz (Hobbs 1984; Cordier & Doukhan 1991) and other minerals including olivine, [$(Mg/Fe)_2$ SiO_4] where the nature and mechanisms of water dissolution are of considerable geochemical significance (Miller *et al.* 1987; Bell & Rossman 1992; Bai & Kohlstedt 1992). There is nevertheless relatively little knowledge of the atomistic structures and reaction mechanisms involved in water and hydrogen dissolution in these materials. In this paper we describe the types of defect and defect reactions which may occur when hydrogen is incorporated in oxide and silicate systems and then show how computational techniques – both simulations, based in interatomic potentials and *ab initio* quantum mechanical techniques – may provide valuable quantitative information as to both the structure and stabilities of the hydrogen containing defects and to the energetics of the corresponding defect reactions. The emphasis of this paper is on bulk defect species; although the importance of hydroxyl groups at surfaces is well known as illustrated by, for example, recent studies of the surface structure of the industrial mineral sodalite (Carr *et al.* 1994).

This study will consider binary oxides (specifically MgO), perovskite structured oxides and a range of minerals, notably quartz, garnets, olivine and microporous catalytic aluminosilicates. We will show how these different classes of oxidic compound exhibit different facets of hydrogen containing defect chemistry.

Phil. Trans. R. Soc. Lond. A (1995) **350**, 265–276

Printed in Great Britain

TEX Paper

2. Reaction mechanisms

Let us consider first the mechanisms whereby water may dissolve in these materials, for which there are the following five broad classes of reactions. In describing these the Kröger–Vink notation will be used (Kröger & Vink 1956; Kingery *et al.* 1976):

(i) *Interstitial formation*

$$(\mathrm{H_2O})_\mathrm{g} \rightarrow (\mathrm{H_2O})_\mathrm{I},$$

in which the water is incorporated at an interstitial site without reaction. This simple process may be of considerable importance in more open structures, especially zeolitic materials, and may be of significance in quartz.

(ii) *Reaction with oxygen vacancies*

$$\mathrm{O_O} + \mathrm{V_O^{\cdot\cdot}} + \mathrm{H_2O} \rightarrow 2\mathrm{OH^{\cdot}}.$$

Here, an incoming water molecule fills an oxygen vacancy creating an OH group after donation of a proton to another oxygen ion.

(iii) *Hydrolysed cation vacancy formation*

$$\mathrm{M_M} + n\mathrm{O} + \tfrac{1}{2}n\mathrm{H_2O} \rightarrow [\mathrm{V_M}^{n+}(\mathrm{OH}_n] + \mathrm{MO}_{n/2},$$

where n is the charge state/valence of the cation. In these reactions, cations are displaced to the surface to form new oxide material and the appropriate number of surrounding oxygen ions are protonated (by the dissolution of water molecules) to achieve electroneutrality.

(iv) *Bridging oxygen hydrolysis*

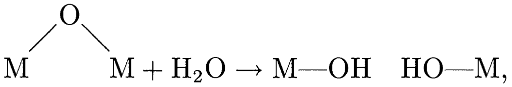

$$\mathrm{M}\overset{\mathrm{O}}{\wedge}\mathrm{M} + \mathrm{H_2O} \rightarrow \mathrm{M{-}OH} \quad \mathrm{HO{-}M},$$

in which water attacks an oxygen bridging two metal atoms in a framework structure, e.g. a silicate, with resulting bond rupture and the creation of two hydroxyl groups.

(v) *Protonation of basic sites*

$$\mathrm{A'_M} + \mathrm{O_O^{\mathit{x}}} + \mathrm{H_2O} \rightarrow (\mathrm{A\ OH}) + \mathrm{OH^-},$$

where A corresponds to a low valence substitutional creating an effective negative charge which enhances the basicity of the neighbouring oxygen site which may then accept a proton from a water molecule. The remaining hydroxyl group is likely to occupy a nearby position in the structure.

We should contrast these mechanisms with those operative for hydrogen molecule incorporation for which we propose three principal classes of mechanism:

(i) *Interstitial formation*

$$(\mathrm{H_2})_\mathrm{g} \rightarrow (\mathrm{H_2})_\mathrm{I},$$

which is of course exactly analogous to the corresponding reaction involving water, unlike the case for the following two incorporation mechanisms, which involve oxidative processes.

(ii) *Oxidation of hydrogen with hole annihilation*

$$2\mathrm{h}^{\bullet} + 2\mathrm{O}_0 + \mathrm{H}_2 \rightarrow 2(\mathrm{OH})^{\bullet},$$

which requires the presence of excess holes due to acceptor impurities. Alternatively we may have:

(iii) *Oxidation of hydrogen by electron creation*

$$2\mathrm{O}_0 + \mathrm{H}_2 \rightarrow 2(\mathrm{OH})^{\bullet} + 2\mathrm{e}',$$

which will of course necessitate the presence of low energy states for conduction band electrons.

We should emphasize the contrast between these *redox* processes compared with the *protonation* acid/base reactions involved in water incorporation. The remainder of this paper will concentrate on the latter reactions; but the theoretical and computational approaches described are generally applicable.

3. Theoretical methods

We use both simulation methods (i.e. techniques based on interatomic potentials) and quantum mechanical approaches to calculate structures and energies of defect configurations. The simulations employ the widely used Mott–Littleton approach (Mott & Littleton 1938; see also Catlow & Mackrodt 1982) in which a region of the crystal surrounding the defect (containing typically 200–400 atoms) is relaxed to zero force, while the surrounding more distant region is treated by quasi-continuum approaches which calculate accurately the polarization of the crystal. There is abundant evidence (Harding 1990) that such methods yield accurate values for formation energies and equilibrium geometries of closed shell defects, provided good interatomic potentials are available; potential models will be discussed in the next section.

The quantum mechanical studies were based on large clusters representing the defect and surrounding lattice. These calculations were confined to our studies of defects in quartz (although the techniques are much more generally applicable). Explicit *ab initio* calculations were therefore performed on clusters with the Si and O atoms in their experimentally determined positions (Levien *et al.* 1980). In all the clusters the Si atoms were tetrahedrally coordinated to oxygen; the surface oxygen atoms were terminated with H atoms (the O–H distance was set to 1.0 Å). A local density functional (LDF) pseudopotential method was used (Jones 1988, 1989) utilizing a basis of s, p- Gaussian orbitals for the valence orbitals. The Schrödinger equation was solved iteratively until self consistency was achieved and the forces on the atom cores evaluated. The atoms were moved using the conjugate gradients method until the net forces vanished.

4. Interatomic potentials

In our simulation studies we used standard, Born model potentials supplemented in the case of the silicate systems by bond-harmonic, three-body terms applied to

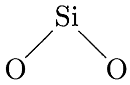

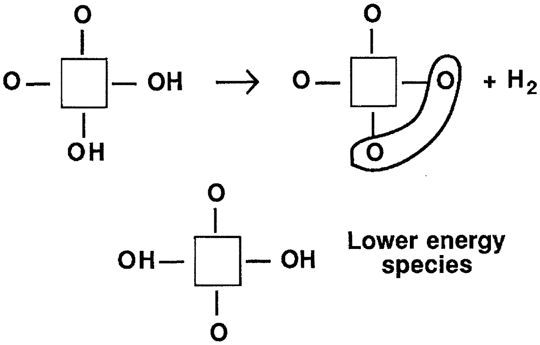

Figure 1. Cation vacancy – hydroxyl clusters in MgO. The proposed mechanism of H_2 loss for the nonlinear cluster is indicated.

bond angles. A shell model treatment of the polarizability of the oxygen ion is included. The parameters for the interatomic potentials have generally been derived by empirical fitting procedures and are reported by Wright & Catlow (1994) and Sanders *et al.* (1984). Special attention should be paid to the potential for the OH group, which plays a key role in this study. Following work of Saul (1985), a Morse potential,

$$V(r) = D\{1 - \exp[-\beta(r - r_e)]\}^2,$$

was used to describe the intramolecular potential energies of this species. The charges for the O and H atoms were chosen so as to reproduce the experimental dipole moment of the OH radical. We also included a shell model description of the polarizability of the oxygen component of the OH group. Modified short range potentials acting between metal ions and this oxygen species were derived as discussed by Wright & Catlow (1994).

5. Case studies

(*a*) MgO

The relevant reactions here are oxygen vacancy filling and hydrolysed cation vacancy formation, which we can represent as follows:

$$V_O^{\cdot\cdot} + O_O + H_2O \rightarrow 2OH^{\cdot},$$

$$Mg_{Mg} + 2O_O + H_2O \rightarrow [V_{Mg}(OH)_2] + MgO.$$

The hydrolysed cation vacancy has two possible structures as shown in figure 1. Calculations indicate that the linear structure has a lower energy, and the reaction energetics reported subsequently are based on the calculated energy for this species. We note that an interesting decomposition mechanism, also shown in figure 1, has been suggested by Freund (1989) for the nonlinear species; it involves loss of a hydrogen molecule with resulting creation of a peroxy ion trapped at the cation vacancy.

Evaluation of the energies of reaction requires use of Born–Haber cycles in which the energy of the proton transfer reaction: $O^{2-} + H_2O \rightarrow 2OH^-$, plays a key role. The latter energy is taken from standard thermochemical data, as discussed by Wright & Catlow (1994) where there are also further details of the

Table 1. *Defect and reaction energies in* MgO
(From Lewis 1995.)

A	Calculated defect energies (eV)	
	magnesium vacancy (V''_{Mg})	23.91
	oxygen vacancy ($V_O^{\bullet\bullet}$)	24.61
	substitutional hydroxyl ($OH^{\bullet}$)	19.65
	hydrolysed cation vacancy [$V_{Mg}(OH)_2$]	56.46
	lattice energy of MgO	−40.91
B	Reaction energies (eV)	
	(1) hydrolysed cation vacancy formation	
	$Mg_{Mg} + 2O_O + H_2O \rightarrow [V_{Mg}(OH)_2] + $‘MgO’	$E = 5.81$ eV
	(2) oxygen vacancy filling	
	$V_O^{\bullet\bullet} + O_O + H_2O \rightarrow 2OH^{\bullet}$	$E = 4.95$ eV

construction of the thermodynamic cycles. Table 1 reports the relevant defect energies, obtained from our Mott–Littleton calculations, together with the resulting calculated reaction energies. We find positive energies of greater than 5 eV for both reactions. We conclude therefore that even in the presence of ‘acceptor’ impurities, such as Li^+, which promote oxygen vacancy formation, water solubility will be low in MgO. Very low levels of OH and of [$V_{Mg}(OH)_2$] species would, however, be expected at higher temperatures. We note also that the latter species is very strongly bound with the energy required to effect dissociation into component V''_{Mg} and $OH^{\bullet}$ defects being *ca.* 3.5 eV.

(*b*) *Hydrogarnet*

This system acts as a test case for the ability of our methodologies to investigate vacancy defects in silicates. The hydrogarnet structure contains hydrolysed silicon vacancies. We therefore calculated the energetics of formation of these species in the grossular end member of the series (i.e. $Ca_3Al_2Si_3O_{12}$). The reaction involved can be represented as

$$Si_{Si} + 4O_O + 2H_2O \rightarrow [V_{Si}(OH)_4].$$

The relevant defect reaction energy is calculated as *ca.* 0.5 eV per water molecule. This low value is compatible with the ready solution of water into this material to form the hydrogarnet species. The energy-minimized structure for this defect is close to that determined by crystallographic studies of hydrogarnet as discussed by Wright *et al.* (1994).

(i) *Quartz*

The question of the mechanism of water incorporation in SiO_2 quartz has been extensively debated (see, for example, Hobbs 1984; Cordier & Doukhan 1991). Several reactions are possible, of which the following are the most important: (i) hydrogarnet defect formation, (ii) bridging oxygen hydrolysis (leading to the formation of the so-called ‘Griggs defect’), (iii) the incorporation of water molecules in the channels of the quartz structure, and (iv) oxygen vacancy filling. The presence of water related species is also important when considering the oxidation

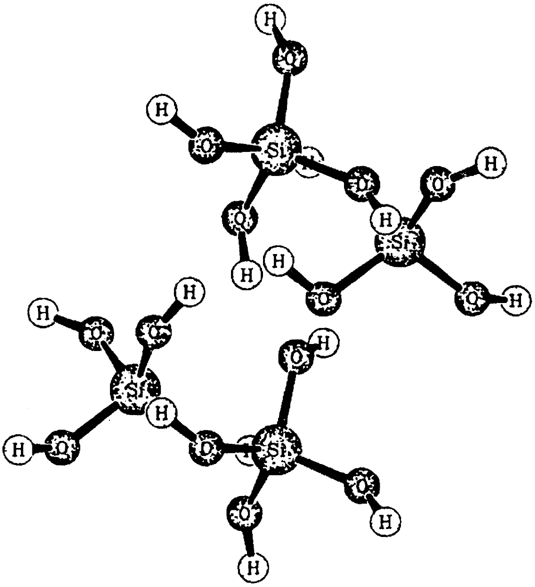

Figure 2. The calculated equilibrium geometry for the hydrogarnet defect.

of silicon metal (Hagon *et al.* 1967*a*, *b*) and the dissolution of minerals (Lasaga 1992).

McLaren *et al.* (1983) and Cordier *et al.* (1988) have observed water precipitation on heating of hydrous α-quartz. The development of bubbles is associated with the formation of sessile dislocation loops and mechanical weakening. Both McLaren *et al.* and Cordier *et al.* have postulated that the hydrogarnet defect may be a precursor and act as a seed for bubble growth. However, Cordier *et al.* could not preclude the possibility that tiny water bubbles (interstitial water) were present and that heating causes diffusion and growth of bubbles at the expense of others.

Purton *et al.* (1992) performed LDF cluster calculations, described above, to determine the structure of the hydrogarnet defect within α-quartz. They took an $Si_5O_{16}H_{12}$ cluster constructed so that a Si atom lay at the centre. This central silicon atom was removed and each of the four surrounding oxygen atoms were protonated. The defect cluster was then relaxed to give the equilibrium configuration in figure 2. The resulting configuration is consistent with that observed in the crystallographic studies of the hydrogarnet structure referred to above. The H atoms lie outside the volume of the oxygen tetrahedron and each H is associated with one face of the O tetrahedron. Thus two O–H distances can be observed – one at 0.99 Å and another at 1.87–1.92 Å.

LDF cluster calculations were also performed on a 54-atom ($Si_8O_{26}H_{20}$) cluster constructed to simulate the 'Griggs defect' (Heggie *et al.* 1994, personal communication). The central bridging oxygen atom was hydrolysed as discussed in § 2. The equilibrium structure obtained has the two hydroxyl groups in a plane with the hydrogen atoms pointing away from one another. By calculating the total energy of the cluster containing the 'Griggs' defect and that of a cluster of ideal quartz and an isolated molecule, an energy for the hydrolysis of the bridging oxygen bond was determined to be 2.3 eV. Further calculations involving larger clusters (approximately 150 atoms) are being undertaken to exclude effects due to boundary conditions.

Atomistic simulations were performed on the hydrogarnet and 'Griggs' defects in α-quartz and in both cases an equilibrium geometry similar to the *ab initio* calculations was observed. One advantage of the atomistic simulations is that defect formation energies are readily obtainable. Furthermore, because of the consistent nature of the parameters used, we may compare the two formation energies in order to determine which of the competing species is likely to be the most stable. The defect reaction energies for formation of the hydrogarnet and 'Griggs' defects are 2.86 and 3.52 eV per H_2O indicating that the hydrogarnet defect is the more stable. We have also performed the atomistic simulation calculations at varying temperatures and pressures from zero temperature pressure up to 500 K and 10 kbar, simulating the experimental conditions. The results show that the volume of formation per water molecule is much greater for the hydrogarnet than the Griggs defect, i.e. at 300 K the formation volumes are 23.2 $\text{Å}^3/H_2O$ and 10.0 $\text{Å}^3/H_2O$ respectively. Therefore, we might anticipate that applying large hydrostatic pressures would favour Griggs defect formation. Further work is, however, needed on this problem.

If 'acceptor' (i.e. low valence) cationic impurities such as Al, are present, incorporation of water by oxygen vacancy filling becomes a possibility. We therefore investigated the energetics of this reaction,

$$O_O + V_O^{\bullet\bullet} + H_2O \rightarrow 2OH^{\bullet},$$

for which we calculated a negative energy (-2.01 eV). Thus in the presence of even low partial pressures of water vapour, Al impurities in quartz will in effect be compensated by OH species. An extensive study of these species was reported by Sim & Catlow (1989). They found that the proton is strongly stabilized on oxygen sites adjacent to the Al; its energy on more distant sites is *ca.* 1.8 eV higher. Interestingly the proton can be exchanged for other cation species, e.g. Li^+ and Na^+.

Finally we should consider dissolution of water molecules in the channels of the quartz structure. Quantum mechanical studies of the structures and energies of water molecules in quartz were reported by Hagon *et al.* (1987*a*, *b*). Energies of *ca.* 2 eV were calculated for the dissolution energy suggesting that such processes could be significant.

(*c*) *Olivine*

The extent of water solubility in olivine has been extensively debated, as has the nature of the resulting defect species (Miller *et al.* 1987; Bell & Rossman 1992; Bai & Kohlstedt 1992). Let us consider first the three obvious reactions; i.e. hydrogarnet defect formation, vacancy filling and hydrolysed magnesium vacancy formation, for which the calculated energies per incorporated water molecule are given in table 2.

The energies of reaction for the formation of the two hydrolysed vacancy defects are high (greater than 3 eV per water molecule). Oxygen vacancy filling is again an exothermic process; but since this material is not normally significantly contaminated with acceptor impurties, oxygen vacancy concentrations are expected to be low.

Table 2. *Defect reactions for* $\mathrm{H_2O}$ *incorporation in olivine*

(1)	hydrogarnet defect formation: $2\mathrm{H_2O}+\mathrm{Si_{Si}} \rightarrow [\mathrm{V_{Si}(OH)_4}]+\text{‘}\mathrm{SiO_2}\text{’}$	$E = 6.1$ (=3.05 per $\mathrm{H_2O}$)
(2)	vacancy filling: $\mathrm{O_O}+\mathrm{V_O}+\mathrm{H_2O} \rightarrow 2\mathrm{OH}^{\cdot}$	$E = -1.24$
(3)	hydrolysed cation vacancy formation: $\mathrm{Mg_{Mg}}+2\mathrm{O_O}+\mathrm{H_2O} \rightarrow [\mathrm{V_{Mg}(OH)_2}]+\text{‘}\mathrm{MgO}\text{’}$	$E = 3.7$
(4)	reduction of Fe^{3+} with protonation of oxygen: $2\mathrm{Fe_{Mg}}+2\mathrm{O_O}+\mathrm{H_2O} \rightarrow 2\mathrm{Fe}^{\cdot}_{\mathrm{Mg}}+2\mathrm{OH}^{\cdot}+\frac{1}{2}\mathrm{O_2}$	$E = 0.46$

We therefore considered a fourth possible mechanism for the solution of water in this material. It involves a redox process in which Fe^{3+} at a magnesium site (a species which is known to be present in appreciable concentrations) is reduced to Fe^{2+} by the dissolving water, i.e.

$$2\mathrm{Fe}^{\cdot}_{\mathrm{Mg}} + 2\mathrm{O_O} + \mathrm{H_2O} \rightarrow 2\mathrm{Fe_{Mg}} + 2\mathrm{OH}^{\cdot} + \tfrac{1}{2}\mathrm{O_2},$$

for which the calculated energy of 0.46 eV is substantially lower than that calculated for formation of either of the hydrolysed cation vacancies; and we suggest that this process is the main mechanism of water incorporation in olivine. Our suggestion is consistent with the observed enhancement of water solubility in olivine by iron impurities (Bell & Rossman 1990). Further discussion of these calculations is given by Wright & Catlow (1994).

(*d*) *Perovskite structured oxides*

Acceptor doped materials with the perovskite or related crystal structures are being used increasingly as proton conductors – materials which are of considerable importance in fuel cell technology. Examples are provided by Yb-doped $\mathrm{SrCeO_3}$ (Iwahara *et al.* 1981) and Fe^{3+} doped $\mathrm{KTaO_3}$ (Scherban & Nowick 1991) which show proton conductivity after reaction with water. OH groups are introduced by the standard vacancy filling reaction (the vacancies being present as charge compensators for the dopants). Protons can then migrate between oxygen ions by a tunnelling process. Recent calculations of Cherry *et al.* (1994) have suggested that the barrier for proton transfer between neighbouring oxygen ions is low. Embedded quantum mechanical cluster techniques were used to investigate the processes in $\mathrm{LaAlO_3}$ with the two nearest neighbour oxygens ions and neighbouring Al ions being described quantum mechanically using high quality basis sets. Hartree–Fock CI calculations were performed, and yielded migration barriers of less than 0.1 eV. Tunnelling through such small barriers would be expected to be a rapid process. The activation energy cannot be equated with the barrier energy discussed above; rather, it is associated with the lattice relaxation energy required to create an equivalent environment around both the sites involved in the tunnelling process. Calculations of this energy term are in progress.

(*e*) *Acidic sites in aluminosilicates and related materials*

We have seen that Al-doped quartz will normally contain charge compensating protons present in well defined Al–OH complexes. The same species are found

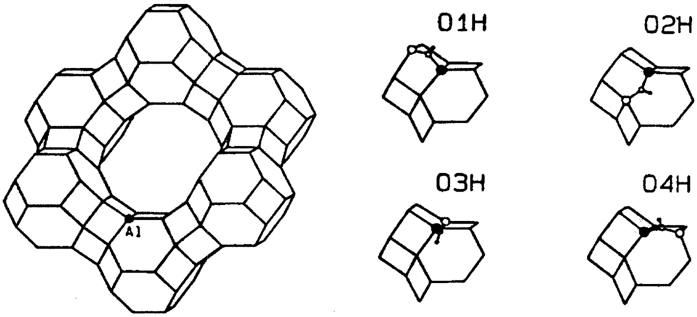

Figure 3. Brønsted acid group in zeolite Y. (*a*) Indicates the Al substitutional site. (*b*) Shows the four possible Al–OH complexes.

in the fascinating group of microporous aluminosilicates known as zeolites which have been extensively studied over many years owing to their unique catalytic properties (see Thomas 1993; Newsam 1992). Much of the catalytic behaviour of these materials can be attributed to the presence of Brønsted acid centres; the micropous architecture, however, controls the nature of the reactions and products giving rise to the phenomenon of shape selective acid catalysis. For this reason the properties the Brønsted acid centres in these materials have been intensively studied by both theoretical and experimental techniques. For example, work of Schroder *et al.* (1992) used Mott–Littleton techniques to characterize the Al–OH centre in Zeolite Y – the widely used hydrocarbon cracking catalyst. The structures of these defects are shown in figure 3; calculations of vibrational frequencies of the OH group are in good agreement with the experimental data. Quantum mechanical techniques have also been extensively used in modelling acid centres in zeolites and their interaction with small molecules (see, for example, the review of Sauer (1992), and the recent work of Gale *et al.* (1993)).

An interesting variant on the theme of acidic centres in microporous materials is provided by the use of Fe^{3+} rather than Al as the substituent for Si. There has been considerable interest in the Fe/ZSM-5 system; the zeolite ZSM-5 has an important role in both catalytic isomerization and hydrocarbon synthesis. Calculations of Lewis *et al.* (1994) demonstrated the stability of the Fe–OH Brønsted acid centre shown in figure 4. The detailed geometry also accords well with the analysis of the Fe K-edge EXAFS spectra of Axon *et al.* (1991). The binding energy of the proton to the site neighbouring Fe is calculated as *ca.* 0.5 eV higher than that for the corresponding Al containing complex – a result that is consistent with the lower acidity of the Fe ZSM-5.

There has also been speculation on the role of hydrogarnet defects (referred to in the context of zeolite science as 'proton nests') in these solids. Further experimental and theoretical studies will be needed to assess the importance of such species in Zeolites.

6. Summary and conclusion

This paper has illustrated the important and pervasive nature of hydrogen containing defects in oxide materials. It has also demonstrated the significant

PHILOSOPHICAL TRANSACTIONS OF THE ROYAL SOCIETY A MATHEMATICAL, PHYSICAL & ENGINEERING SCIENCES

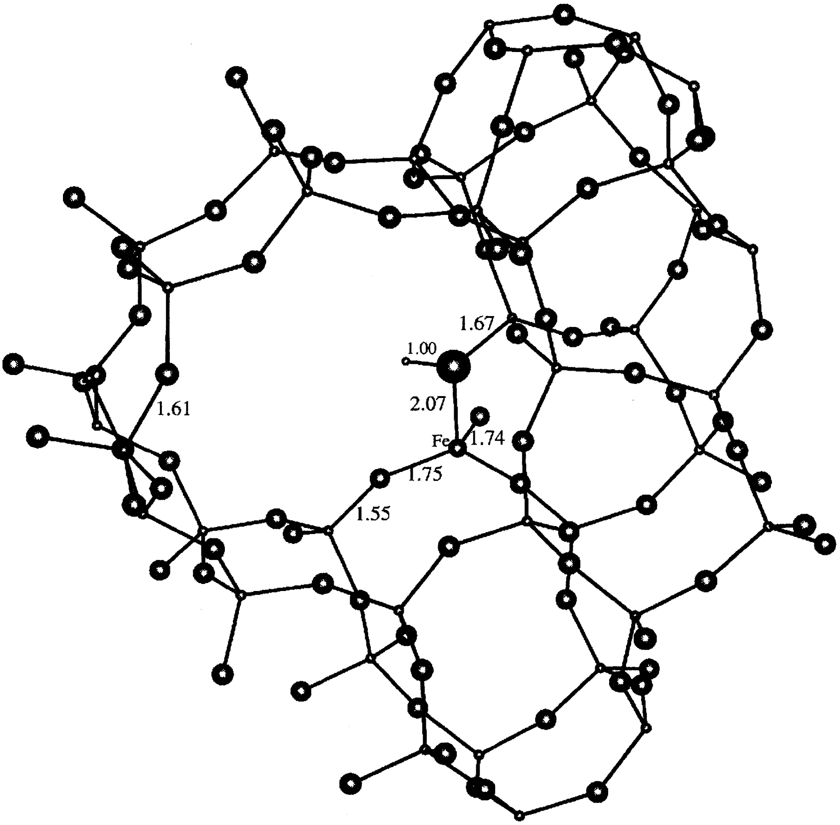

Figure 4. Fe–OH, Brønsted acid site in Fe ZSM-5 (geometries with bond lengths in Å obtained by using Mott–Littleton techniques by Lewis *et al.* 1994).

contribution which can be made by theoretical and computational techniques in advancing our understanding of these complex defects.

We are grateful to several colleagues for useful discussion, notably A. M. Stoneham, J. M. Thomas, G. D. Price, R. Freer, D. W. Lewis, S. Carr, M. Cherry and M. S. Islam. We are also grateful to R. Jones and M. Heggie for permission to quote unpublished results.

References

Axon, S. A., Fox, K. K., Carr, S. W. & Klinowski, J. 1992 *Chem. Phys. Lett.* **189**, 1–6.

Bai, Q. & Kohlstedt, D. L. 1992 *Nature, Lond.* **357**, 672.

Bell, D. R. & Rossman, G. R. 1990 *Science, Wash.* **225**, 1391.

Catlow, C. R. A. & Mackrodt, W. C. (eds) 1982 *Computer simulation of solids.* Lecture Notes in Physics, vol. 166. Berlin: Springer.

Cherry, M., Islam, M. S., Gale, J. O. & Catlow, C. R. A. 1995 *Solid State Ionics.* (In the press.)

Cordier, P., Boulogne, B. & Doukhan, J. C. 1988 *Bull. Mineral* **111**, 113.

Freund, F. 1989 *Advances in solid state chemistry* (ed. C. R. A. Catlow), vol. I. JAI Press.

Gale, J. D., Catlow, C. R. A. & Carruthers, J. R. 1993 *Chem. Phys. Lett.* **216**, 155–161.

Hagon, J. P., Stoneham, A. M. & Jaros, M. 1987*a* *Phil. Mag.* **55**, 221.

Hagon, J. P., Stoneham, A. M. & Jaros, M. 1987*b* *Phil. Mag.* **55**, 225.

Harding, J. H. 1990 *Rep. Prog. Phys.* **53**, 1403.

Hobbs, B. E. 1984 *J. geophys. Res.* **89**, 4026.

Iwahara, H. 1992 *Solid State Ionics* **53–56**, 575.

Iwahara, H., Esaka, T., Uchida, H. & Maeda, N. 1984 *Solid State Ionics* **3–4**, 359.

Jones, R. 1988 *J. Phys.* C **21**, 5735.

Jones, R. 1989 *Molec. Simulat.* **4**, 113.

Kingery, W. D., Bowen, H. K. & Uhlmann, D. R. (eds) 1976 *Introduction to ceramics*, p. 127. New York: Wiley.

Kröger, F. A. & Vink, V. J. 1956 *Solid state physics* (ed. F. Seitz & D. Turnbull), vol. 3, p. 307. New York: Academic Press.

Lasaga, A. C. 1992 *Rev. Geophys.* **30**, 269.

Levien, L., Prewitt, C. T. & Weidner, D. J. 1980 *Am. Mineral.* **65**, 920.

Lewis, D. W. 1995 Ph.D. thesis, University of London.

Lewis, D. W., Catlow, C. R. A., Sankar, G. & Carr, S. W. 1995 *J. Phys. Chem.* (In the press.)

Loades, S. D., Carr, S. W., Gay, D. H. & Rohl, A. L. 1994 *J. chem. Soc. chem. Commun.*, p. 1369.

Miller, G. H., Rossman, G. R. & Harlow, G. E. 1987 *Phys. Chem. Minerals* **14**, 461.

Mott, N. F. & Littleton, M. J. 1938 *Trans. Farad. Soc.* **34**, 485.

Newsam, J. M. 1992 In *Solid state chemistry – compounds* (ed. A. K. Cheetham & P. Day). Oxford University Press.

Purton, J., Jones, R., Heggie, M., Öberg, S. & Catlow, C. R. A. 1992 *Phys. Chem. Minerals* **18**, 389.

Sanders, M. J., Leslie, M. & Catlow, C. R. A. 1984 *Chem. Soc. Chem. Commun.* p. 1271.

Sauer, J. 1992 In *Modelling of structure and reactivity in zeolites* (ed. C. R. A. Catlow), p. 183. London: Academic Press.

Saul, P., Catlow, C. R. A. & Kendrick, J. 1985 *Phil. Mag.* B **51**, 107.

Scherban, J. & Nowick, A. S. 1992 *Solid State Ionics* **53–56**, 1004.

Schröder, K.-P., Sauer, J., Leslie, M., Catlow, C. R. A. & Thomas, J. M. 1992 *Chem. Phys. Lett.* **188**, 320.

Sim, F. & Catlow, C. R. A. 1989 *Int. J. quant. Chem. quant. Chem. Symp.* **23**, 651.

Thomas, J. M. 1992 *Scient. Am.* **266**, 85–88.

Wright, K. V. & Catlow, C. R. A. 1994 *Phys. Chem. Mineral* **20**, 515.

Wright, K. V., Freer, R. & Catlow, C. R. A. 1994 *Phys. Chem. Mineral* **20**, 500.

Discussion

A. M. STONEHAM. (*Harwell Laboratory, Oxfordshire, U.K.*). Professor Catlow gave a very nice survey of hydrogen reactions. Presumably similar reactions determine the fractions of muons which remain as μ^+, which muonium, or which go missing (perhaps by reaction with oxygen). Early data (J. H. Brewer, personal communication 1983) show about 60% muonium formation in SiO_2, but negligible muonium in GeO_2 or SnO_2 (for SnO_2 essentially 100% remains as μ^+ despite the many oxide ions). Can one predict these fractions?

C. R. A. CATLOW. The fraction of muonium is probably strongly influenced by the initial processes occuring when the muon beam interacts with oxide, capturing electrons with hole creation. It may be difficult to make precise predictions relating to these processes. I find it difficult to rationalize the difference Professor Stoneham refers to between the behaviour of SiO_2, GeO_2 and SnO_2 in terms of any simple factors relating to changes in crystal structures or electronic properties. The differences may relate to changes in the relative mobilities of muonium, muons and holes in the three materials.

R. JONES (*Department of Physics, Exeter, U.K.*). Could Professor Catlow expand on the mechanism of catalytic processes involving methanol in zeolites?

C. R. A. CATLOW. The mechanism of catalytic activity of methanol in zeolites remains controversial. What now seems increasingly clear is that initially the methanol is trapped on the Brønsted acid site to which it is strongly H-bonded (see Gale *et al.* 1993). The mechanism whereby the C–C bond formation is initiated is uncertain, although there have been useful discussions based on quantum chemical calculations.

M. SYMONS (*Department of Chemistry and Biological Chemistry, University of Essex, U.K.*). I found the redox process postulated for olivine of considerable interest. In this Professor Catlow invoked Fe(III) impurities, which were changed to Fe(II). It would be easy to check this (UV or ESR), and I wondered if this had been done?

C. R. A. CATLOW. This suggestion is an interesting one which should be followed up. Of course the crucial issue is whether the *changes* in the Fe^{3+}/Fe^{2+} ratio in the material due to the reaction with water could be detected.